Nanometrology of delignified *Populus* using mode synthesizing atomic force microscopy

2011 Nanotechnology 22 465702

(http://iopscience.iop.org/0957-4484/22/46/465702)

Nanotechnology **22** (2011) 465702 (9pp) doi:10.1088/0957-4484/22/46/465702

Nanometrology of delignified *Populus* using mode synthesizing atomic force microscopy

L Tetard[1], A Passian[1,2], R H Farahi[1], B H Davison[1], S Jung[1,3], A J Ragauskas[1,3], A L Lereu[4] and T Thundat[5]

[1] BioEnergy Science Center, Oak Ridge National Laboratory, Oak Ridge, TN 3783, USA
[2] Department of Physics, University of Tennessee, Knoxville, TN 37996, USA
[3] Georgia Institute of Technology, 500 10th Street, Atlanta, GA 30332, USA
[4] CINaM-CNRS UPR 3118, Campus de Luminy, F-13288 Marseille Cedex 09, France
[5] Department of Chemical and Materials Engineering, University of Alberta, Edmonton, AB, T6G 2V4, Canada

E-mail: passianan@ornl.gov

Received 28 June 2011, in final form 5 September 2011
Published 25 October 2011
Online at stacks.iop.org/Nano/22/465702

Abstract
The study of the spatially resolved physical and compositional properties of materials at the nanoscale is increasingly challenging due to the level of complexity of biological specimens such as those of interest in bioenergy production. Mode synthesizing atomic force microscopy (MSAFM) has emerged as a promising metrology tool for such studies. It is shown that, by tuning the mechanical excitation of the probe–sample system, MSAFM can be used to dynamically investigate the multifaceted complexity of plant cells. The results are argued to be of importance both for the characteristics of the invoked synthesized modes and for accessing new features of the samples. As a specific system to investigate, we present images of *Populus*, before and after a holopulping treatment, a crucial step in the biomass delignification process.

(Some figures in this article are in colour only in the electronic version)

1. Introduction

Characterization of structures at the nanoscale without significantly altering their material properties is of great importance in nanotechnology [1]. Furthermore, noninvasive nanometrology is indispensable in the study of live biological specimens or nanoscale soft matter [2]. Similarly, plant biology can profit from high resolution microscopy, for example when investigating the functionality of the internal components of biomass [3]. Plant cells have recently drawn considerable attention due to their importance in biofuel research [4]. A mixture of the organic compounds (i.e. cellulose, hemicellulose and lignin) is contained in the plant cell wall of which the non-lignin components could be a potential abundant source of sugars for conversion to ethanol through a series of processes [5]. Lignocellulosic biomass pretreatment is considered as an essential process in order to increase the conversion of biomass to ethanol product through enabling a more acceptable biomass to the cellulase enzyme process. Lignin is known to be a barrier to impede cellulase efficiency and thus has to be removed for efficient biomass saccharification. Moreover, lignin removal/alteration in lignocellulosic materials is often used as a key factor to determine pretreatment efficacy. The holopulping process has a role of delignification through lignin depolymerization and hydrolysis in the plant cell wall. Subsequent conversion processes include the saccharification of the recovered non-lignin cellulosic material into simple monosaccharides (i.e. sugars), microbial fermentation of the sugars and removal of the ethanol from the fermentation broth. The efficient deconstruction of the lignocellulosic materials from holopulping to harvest the complex sugars for fermentation remains a major challenge in biofuel production due to the plant cell's natural resistance to decomposition, also known as recalcitrance [6].

Nanoscale characterization of cell morphology can provide important structural and chemical information that

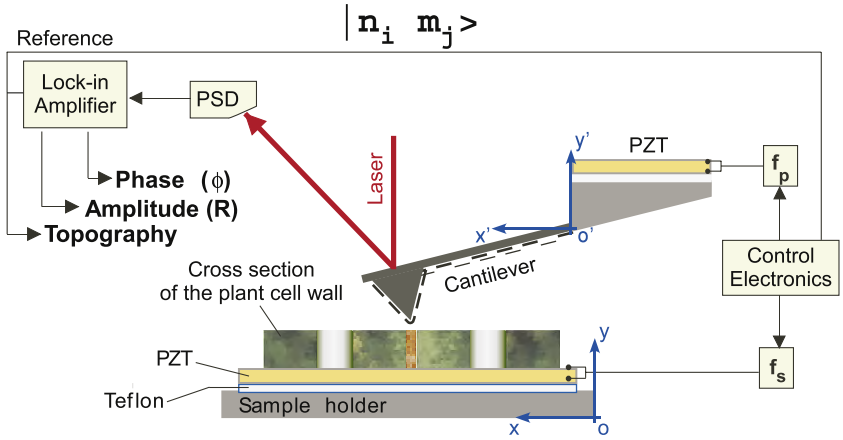

Figure 1. Schematic representation of the experimental set-up used for the measurements. The synthesized modes are labeled as $|n_i m_j\rangle$, with $i, j =$ s, p (for sample and probe), and $n, m = \pm 1, \pm 2, \ldots$ corresponding to a given combination of the excitations that yields the mode.

can aid cellulose-to-alcohol conversion processes [7, 8], as in the holopulping process described here. The dynamic attributes of the atomic force microscopy (AFM) [9], in particular multifrequency AFM [10], have recently been shown to provide powerful new modalities for the study of surfaces and beyond [11]. More recently, introducing the mode synthesizing AFM (MSAFM), shown in figure 1, it has been reported that a more extended exploitation of the nonlinear coupling between the tip of the cantilever and the sample can provide a wealth of information on the physical properties of various materials [12]. A remarkable example herein is the introduction of the concept of virtual resonance as yet another dynamic feature of force microscopy with tremendous potential for subsurface exploration [13]. While a more comprehensive account of the utilization of the virtual resonance for imaging is the subject of forthcoming articles, we here suffice with stating that the dynamic measurements presented here underpin emerging multifrequency force microscopy techniques [14].

Accessing the physical and compositional properties of materials at the nanoscale is both important and challenging in the current state of material characterization [15]. Due to the complexity of the cell wall and small dimensions of its substructures, any noninvasive characterization of such samples could profit from force microscopy with its nondestructive, high resolution capabilities. Microscopy and spectroscopy of biomass have been explored employing a number of probing approaches [7, 8, 16–26]. The AFM methodologies enable the mapping of nanoscale surface features such as biomass morphology or cellulose microfibrils [16–18] by providing a mechanical probe that interacts with the material via atomic forces. The nanoscale features may be investigated using an electron probe as in scanning electron microscopy (SEM) [8, 19, 27] and transmission electron microscopy (TEM), where properties such as the microfibril's orientation or the degrees of porosity of the membranes in hardwood species of biomass have been investigated in relation to wood density and its vulnerability to cavitation [19]. In particular, the development of the environmental SEM mode (ESEM) in recent years has enabled high resolution morphological information on fully hydrated tissues of lignocellulosic biomass, such as Alfalfa stems [20]. ESEM was also employed by Hamm *et al* [20], where the effect of thermal dehydration on wood stems under decreasing vapor pressures was investigated. Such studies could provide information on thermal dehydration and the degree of damage on the poorly lignified cells versus the vessels and fibers richer in lignin. Photon-based probes such as high resolution near-field scanning optical microscopy (NSOM) have also been proposed for surface analysis of biomass if tip-related issues can be resolved [25]. Lower resolution optical methods such as confocal and confocal Raman microscopy have been reported for the study of lignification in wild and transgenic *Populus trichocarpa* stem wood [26]. Schmidt *et al* [26] achieved submicron spatial resolution (within the lignin Raman bands of 1600–1700 cm^{-1}) and reported a decrease in lignin content in the secondary wall of the cell for the transgenic form of the stem. Furthermore, spectroscopic techniques continue to provide valuable chemical and compositional information [25]. Recent studies using UV–visible [28], fluorescence [29], CARS [30] and Raman [26] spectroscopy have provided a host of important investigations ranging from the crystallinity, the sizes of the crystallite of the fibers and the lignin content of the cell walls to the cellulase adsorption during enzymatic hydrolysis of the biomass systems. Other powerful techniques such as time-of-flight secondary ion mass spectrometry (ToF-SIMS) [27] or nuclear magnetic resonance (NMR) [8, 21] are being considered for the investigation of the structure of lignocellulosic biomass [6]. AFM has recently been reported in the effort to characterize the structure of *Populus* cell walls [12]. While the nature of the tip–sample interaction in AFM makes it possible to minimally invasively map the external morphology of various samples with high lateral resolution, the approach is also evolving into a very flexible platform for studying other physical properties of materials. In particular, the coupled oscillations of the tip of the probe and the surface of the sample, facilitated by the attractive and repulsive forces at play in the system [13], can aid in developing novel measurement techniques akin to nanometrology. In MSAFM, by combining

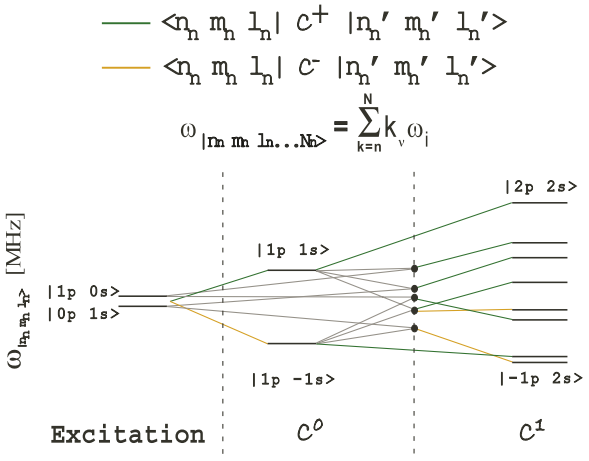

Figure 2. Partial diagrammatic representation of the higher level coupling resulting from the tip–sample interaction in MSAFM. The left axis denotes the frequency. The green lines denote modes created via sum frequency generation, while the orange lines correspond to those created via difference frequency generation. The modes arranged in the middle and the last columns are due to first-order and higher-order couplings, respectively. Only mode groups relevant in this work are expanded.

AFM with ultrasonic microscopy [31–33], a rich spectrum of new oscillations or modes can be created in the coupled probe–sample system due to the nonlinear interfacial forces [11, 12]. The myriad of new modes exhibited by the system can be categorized in a level diagram similar to the graphic representation of the atomic energy levels and allowed transitions (figure 2). The diagram helps visualize the complex sequence of mode synthesization. The modes have been demonstrated to be functional for imaging [12] and provide important and complementary information on the surface and subsurface properties of the sample [11, 12] not otherwise attainable. In this work, by comparing the MSAFM images of the individual cross sections after each chemical treatment, we report it is possible to get better information on how the different cell wall components respond to the chemical processes and to determine the composition of the cell wall.

2. The concept of mode synthesizing

While a comprehensive analytical treatment of the MSAFM problem is outside the scope of the current work, the underlying dynamics may be exposed by formulating the probe–sample interaction in a moving coordinate system o′, in which the fixed ($x' = 0$) boundary of the probe is stationary, as shown in figure 1. The partial differential equation for the elastic wave propagation in the microcantilever (length l) of the AFM can be shown, in the o′ system, to take on the form $\mathcal{L}_c u(x', t') = F(x', t')$, where $\mathcal{L}_c$ is the differential operator, within the Euler–Bernoulli theory, for the transverse oscillations u of the probe [34] in response to a force F. Transforming to the o system, we note that an imposed oscillation at o′ such that the time-varying position $\bar{r}_{o'} = (0, y)$ with an arbitrary form $y = f(t)$, will appear, in the o system, as a driving force (probe excitation) such that one arrives at $\mathcal{L}_c u(x, t) = \alpha \ddot{f}(t) + \beta \dot{f}(t) + F(x, t)$, where α and β are constants that contain the material properties of the probe. With $F = F(x, t)$ this problem can be solved analytically by an eigenfunction expansion [34]. However, solving the problem for the case of figure 1, is considerably more complicated as it requires the introduction of a nonlinear probe–sample interaction mandating a functional form for the force $F = F[u(x, t), t]$. Denoting the free end of the probe with $\bar{r}_l$, the dynamics is further complicated by the introduction of the sample excitation as the interaction force will depend on a gap size $d = d(t) = |\bar{r}_l - \bar{r}_s| = |u(l, t) - v(r_s, t)|$ that is being modulated. Here, $v(r_s, t)$ is the dynamic state of the interrogated sample point $\bar{r}_s$. Representing the sample dynamics at point $\bar{r}_s$ as a damped harmonic oscillator (DHO), we may write

$$\mathcal{L}_c u(x, t) = \alpha \ddot{f}(t) + \beta \dot{f}(t) + F(d)$$

$$\mathcal{L}_s v(t) = g(t) + G(d)$$

where G, proportional to F, is the interaction force on the sample, $\mathcal{L}_s$ is the DHO differential operator and $g(t)$ is a driving force exerted from the fixed (immobilized on a piezoelectric substrate) boundary of the sample. For the samples used here G may safely be neglected (the sample being constrained at the interface with the piezoelectric substrate). However, in the general case, by resorting to heuristic arguments it can be surmised from the structure of the coupled equations above that the frequency content of the resulting dynamics, that is, $u(x, \omega)$ the Fourier transform of $u(x, t)$, will be a function of the frequency contents of both functions $f(t)$ and $g(t)$. Furthermore, the forms of $F(d)$ and $G(d)$ will affect the spectral distribution of $u(x, \omega)$. Therefore, it is reasonable to assume that formally oscillation parameters at each frequency component of $u(x, \omega)$ may be represented with $\langle X_f | \mathcal{C} | X_g \rangle$, where $|X\rangle$ represents the excitation state at the frequency of f or g, while $\mathcal{C}$ denotes a general coupling. We recently reported the experimental observation of the action of $\mathcal{C}$ [12] and showed that if a semi-empirical nonlinear force is assumed to represent the probe–sample interaction ($\propto F$), then one can show that frequency difference generation can occur in agreement with the experimental measurements [13].

The subsurface capability of MSAFM may be understood if the sample is envisioned as being composed of a lattice $i, j = 1, 2, 3, \ldots$ of DHOs [35], each with a set of coefficients for $\mathcal{L}_s$. Then, the dynamics can be modeled by the system

$$\mathcal{L}_c u(x, t) = \alpha \ddot{f}(t) + \beta \dot{f}(t) + F(d).$$

$$\mathcal{L}_s^{ij} v(t) = g(t), \qquad i, j = 1, 2, 3, \ldots.$$

Similarly, it can be shown that, with a stationary sample, d can be brought into modulation by a multiple N frequency linear forcing such that $f(t) = \sum_{n=1}^{N} f_n(t)$, $n = 1, 2, 3, \ldots$ and thus the probe response would be the solution of

$$\mathcal{L}_c u(x, t) = F(|u(l, t) - v_{ij}(0)|) + \sum_{n=1}^{N} \left[\alpha \ddot{f}_n(t) + \beta \dot{f}_n(t)\right],$$

where $v_{ij}(0)$ represents the topography of the sample. For each i, j, the nonlinear force $F_{ij} = F(d_{ij})$ mixes the frequencies $\omega_n, n = 1, 2, 3, \ldots, N$, as shown in figure 2. The experimental observation and practical applications of this effect will be reported elsewhere.

With this prelude to the underlying mechanism of the MSAFM, we proceed to demonstrate how this multifrequency force microscopy successfully accesses new information by imaging a set of samples of the cross sections of *Populus* wood, before and after holopulping treatment. Understanding the chemically and morphologically complex *Populus* wood and other plant cells is currently of prime interest for biomass conversion [6, 36, 37]. However, an accurate model of the organization (e.g. chemical, structural, etc) of biomass at the subcellular level is still missing, thus slowing progress towards overcoming recalcitrance [6, 38, 39]. Standard analytical techniques have been used to gather a complementary set of information on the plant cell wall, aiming at a deeper understanding that could be applied to further optimization of the processes of biofuel production.

3. Experimental procedures

The experimental set-up is sketched in figure 1. For a brief motivation and need for resorting to multifrequency techniques such as the MSAFM concept and the state of force microscopy, reference can be made to a recent article by Garcia [15]. Experimentally, a typical MSAFM session begins with driving the cantilever probe of an AFM into high frequency oscillation using a piezoelectric crystal (PZT). Similarly, the sample is mounted on another PZT for mechanical excitation. The mechanical response of the probe to the combined effect of forced base oscillations and sample-induced tip modulations is monitored in time and frequency domains using a high bandwidth oscilloscope and spectrum analyzer. After a preliminary analysis of the frequency content of the signal, lock-in detection is engaged to yield a complex signal, which can be studied with respect to its amplitude R and phase φ at the selected frequencies. For this purpose, an AFM[6] was adapted in the present study. The signal was extracted through a signal access module (see footnote 6) for lock-in measurements, and rerouted to the AFM controller to display the corresponding map of the signal. In the final configuration, the AFM is operated as an ultrasonic-based MSAFM [12], using a set of mechanical excitations of the probe $|X\rangle = \sum_{n=1}^{N} a_n \sin(\omega_n t + \varphi_n)$ and another set of excitations of the sample $|X'\rangle = \sum_{n=1}^{N'} a'_n \sin(\omega'_n t + \varphi'_n)$. In this first phase of trials, the excitations in the form of a monoharmonic or multiharmonic waveform were mechanically induced using driven piezoelectric bimorphs. Standard procedures for AFM imaging in contact mode can then be implemented to acquire a signal for imaging. As shown in figure 1, when the tip and the sample are in contact, the signal $S(t)$ is analyzed in time and in Fourier domains. The evolution of each of the modes of the system, observed as a set of peaks using a spectrum analyzer, can further be individually monitored and selected for imaging using a lock-in amplifier. Both the amplitude R and the phase φ of the output signal can then be plotted in the form of a two-dimensional map, for comparison with the simultaneous topography image [12]. This procedure can thus be repeated for any number of synthesized modes, each (for the case $N = N' = 1$) being symbolically denoted as $|n_s m_p\rangle$, where s and p denote the sample and the probe, respectively, and n and m correspond to their respective frequency contribution, such that $f_{|n_s m_p\rangle} = n f_s + m f_p$.

We evaluated two sets of the sectioned biomass samples: fresh *Populus* and holopulped *Populus*, each typically 50 μm thick and less than a centimeter in diameter. *Populus deltoides* stems were grown at the National Renewable Energy Laboratory (NREL) and harvested between 2007 and 2008. The stems were then stored at $-20°$ [27]. The samples were prepared using chemical treatments that simulate some pretreatment chemistries involved in biomass conversion to biofuel. The motivation behind using this plant system was to obtain information on the effectiveness of the holopulping process through high spatial resolution analysis of the altered cell wall structures. A whole poplar stem (Juvenile *Populus deltoides*) was sectioned into 50 μm thickness samples using a Leica CM 3050S (Leica Microsystems, Wetzlar, Germany) equipped with a disposable steel blade [27]. To avoid chemical contamination from the embedding medium, the sample was directly attached to the metal stage, instead of embedment, and sectioned. Cross sections of poplar stems were examined instead of the usual sawdust or milled wood, in order to aid the structural analysis during the imaging measurements. Previous work by Jung *et al* [27], where this specific sample preparation is discussed, verified by means of spectroscopic measurements that the chemical modifications undergone by the cross sections are comparable to that of the 20-mesh ground (milled) poplar material usually used for larger scale studies. Extractives in the cross section of *Populus* stems were removed by sequential Soxhlet extractions in order to obtain a section of extractive-free poplar. The section of extractive-free poplar was subjected to an oxidative treatment to prepare a section of holocellulose poplar following literature protocols [40, 41]. In brief, the section of extractive-free poplar was dispersed into deionized (DI) water (100 ml g^{-1} sample) with sodium chlorite (40% by dry weight of sample) and glacial acetic acid (10% by dry weight of sample) at 70° for 1 h in a sealed plastic pouch (Kapak Corporation, Minneapolis, MN, USA). The procedure was then repeated three additional times. Finally, the solid residue (holocellulose) was filtered out and washed thoroughly with DI water. Both samples, in the form of sections prepared from fresh specimens, were stored in a dry environment between two glass slides. As a result, structural distortion is minimized and the native form of the samples are better maintained. Prior to the measurements, the samples are immobilized on a substrate using thin adhesive films (standard adhesive tabs used for sample attachment in SEM). This procedure allows sufficient coupling and propagation of the PZT-generated ultrasonic waves in the samples.

[6] Commercial AFM system: Multimode from Veeco with a Nanoscope III controller. Signal manipulation via a signal access module from Veeco.

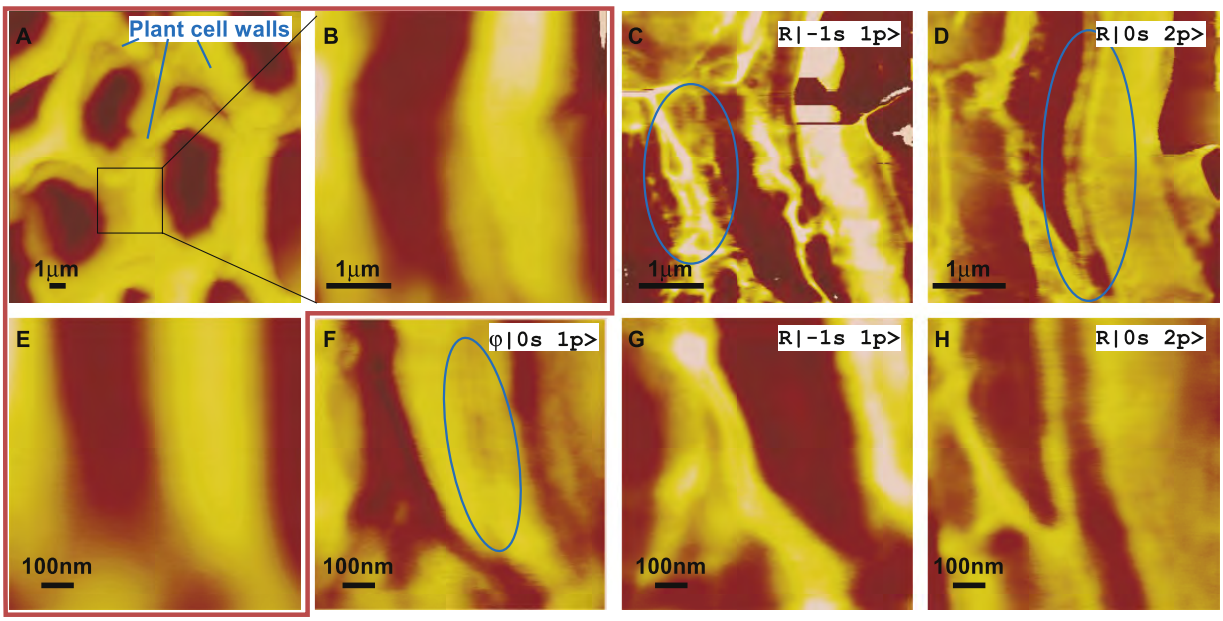

Figure 3. Characterization of the cell walls of fresh *Populus*. (A), (B), (E) Topography AFM images (marked in the red box). (C), (D), (G), (H) The corresponding MSAFM amplitude (R) images reveal nanoscale features of the complex composition of the plant cell walls, which were not accessible with standard AFM microscopy ((A), (B), (E)). For example, vacuole-like structures in (C) or the interface between layers (D) can be observed (see circles). The MSAFM phase φ image (F) also illustrates the interfacial regions between the middle lamella and the cell wall. (E)–(H) correspond to higher resolution images of (B)–(D). MSAFM excitation parameters were $f_{|1_s 0_p\rangle} = 1$ MHz and amplitude $R_{|1_s 0_p\rangle} = 5$ Vpp for the sample, and $f_{|0_s 1_p\rangle} = 1.39$ MHz and $R_{|0_s 1_p\rangle} = 6\ V_{pp}$ for the probe, using the synthesized modes (C) $R_{|-1_s 1_p\rangle}$, (D) $R_{|0_s 2_p\rangle}$, (F) $\varphi_{|0_s 1_p\rangle}$, (G) $R_{|0_s 2_p\rangle}$ and (H) $R_{|-1_s 1_p\rangle}$. The presented MSAFM modes express the mechanical properties, reveal vacuole-like features and indicate stiffness variations in the cell wall (C).

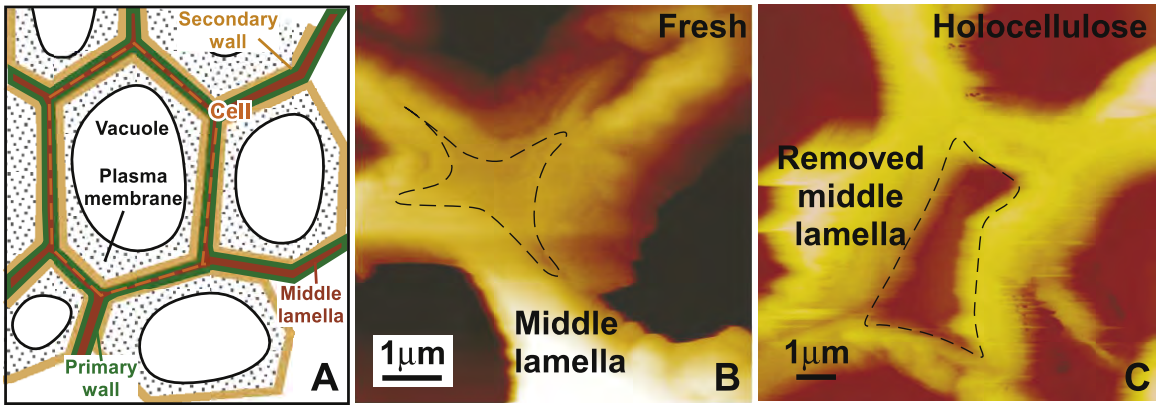

Figure 4. Schematic of the cross section of fresh *Populus* (A) and effect of the chemical treatment on the cell walls (B) and (C). Topography images of the fresh *Populus* (B), and holocellulose *Populus* (C). The chemical treatment contributed to the removal of the middle lamella across the sample as shown in brown in (A), resulting in a change of mechanical properties of the cell walls.

4. Results and discussion

Using the unique phase-sensitive capabilities of MSAFM for imaging materials and detecting changes in physical properties at the nanoscale, we characterized fresh *Populus* cross sections (figure 3) and a similar cross section after holopulping treatment intended to remove the lignin content of the cell wall (figures 4–6). In figure 3 standard AFM topography images are marked with a red outline (A), (B) and (E). MSAFM images acquired simultaneously, respectively (C), (D) and (F)–(H), reveal new nanoscale features of the complex composition of the plant cell walls, which were not accessible with standard AFM. For example, vacuole-like structures in (C) or the interface between layers (D) and (F) could be observed (demarcated with ovals). Higher resolution images of (B) are presented in (E)–(H). (F) and (H) reveal the presence of structures in the cell wall with dimensions of the order of 100 nm, which were not resolved in the topography (E). The rich information in mechanical properties of the cell wall contained in (G) and (H) is a direct indication of the complexity of the organization of the networks of polymers (i.e. lignin, cellulose and hemicellulose) in the cell wall. For this study the

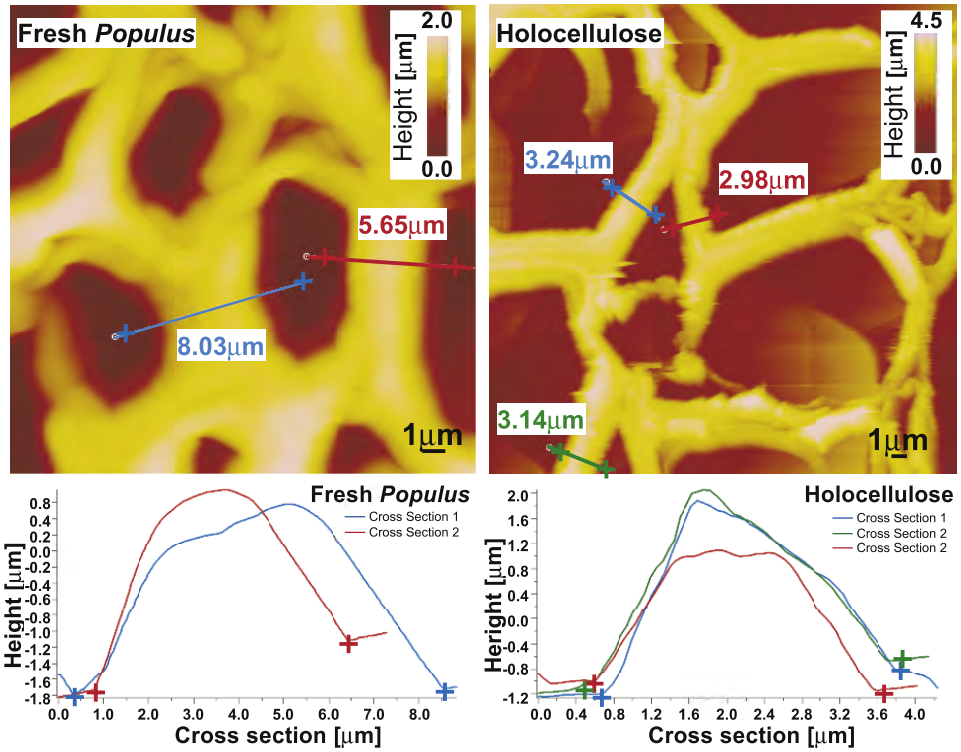

Figure 5. Sections across the cell wall of fresh and treated samples illustrate the effect of holopulping on the cell wall structures. In addition to the removal of the middle lamella across the sample (figure 4), the thickness of the wall tends to decrease. In the topography images presented here, the decrease in the thickness of the cell wall varied from 2 to 5 μm.

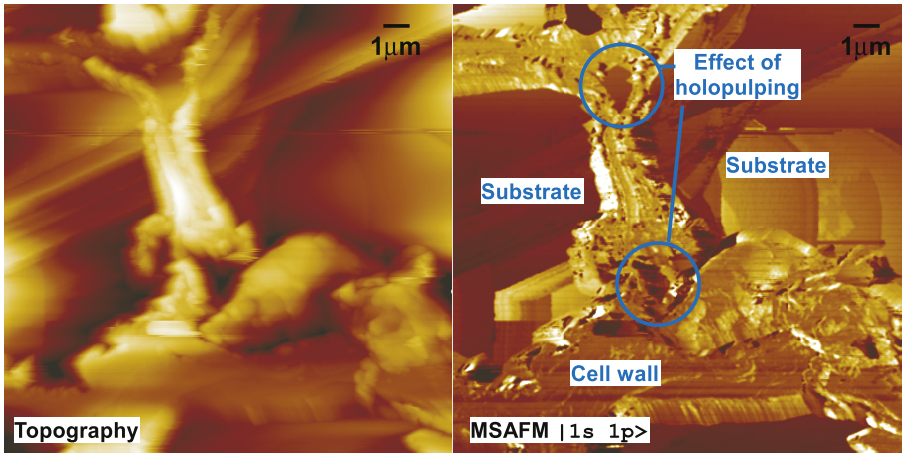

Figure 6. Topography (left) and MSAFM (right) images of holocellulose sample (scale bar 1 μm). The MSAFM image (right) was acquired using the amplitude of the synthesized mode $|1_s1_p\rangle$ with a sample excitation frequency $f_{|1_s0_p\rangle} = 200$ kHz, amplitude $R_{|1_s0_p\rangle} = 1$ V_{pp}, probe excitation frequency $f_{|0_s1_p\rangle} = 50$ kHz and amplitude $R_{|0_s1_p\rangle} = 2$ V_{pp}. MSAFM allows the identification of changes in material (substrate and vacuoles in cell walls).

MSAFM excitation modes were: $|1_s0_p\rangle$ with a frequency of 1 MHz and an amplitude of 5 Vpp corresponding to the sample excitation, and $|0_s1_p\rangle$ with a frequency of 1.39 MHz and an amplitude of 6 V_{pp} corresponding to the probe excitation. As a result a number of operational modes were synthesized with varying amplitudes and phases with the following used for the measurements here: (C) and (G) $R_{|-1_s1_p\rangle}$, (D) and (H) $R_{|0_s2_p\rangle}$ and (F) $\varphi_{|0_s1_p\rangle}$. The high resolution observation of subsurface features revealed by the new modes of the MSAFM provide a complementary source of morphological information when compared to other techniques. For similar samples, such comparisons are feasible for example by SEM images reported by Jung *et al* [27]. The effect of the holopulping treatment on the sectioned samples is illustrated in figure 4, where the area richer in lignin content, consistently observed across the fresh sample cross section presented in (B), seems to be removed in the cross section of holocellulose samples as demarcated by the dashed line in (C). Thus, with reference to the schematics

of the cellular configuration of the cross section shown in (A), the holopulping process, intended to oxidatively remove the lignin network in the cell, appears to affect mostly the middle lamella as well as the cell corner regions. In addition, the cell walls tend to be thinner in holocellulose, indicating a possible role of lignin in the cell wall as well. As described in section 3, it is noted that the samples denoted as fresh and those referred to as holocellulose, are understood to be different. Consequently, when comparing the images presented in figures 4 and 5, we intend to illustrate a trend observable across the samples. In figure 5, a comparison between the cell walls of the fresh sample and the cell walls of the holocellulose sample is made using the AFM topography images. The cross section of the cell wall, taken at the location of the line markers, produces a profile that allows further analysis such as cell wall thickness measurements. As indicated in figure 5, the cell wall before treatment is approximately 8 μm, whereas the measurements indicate 3–4 μm for the holocellulose sample. The overall morphology of the chemically modified sample exhibits changes when compared to the fresh sample, with a significant void appearing in the naturally lignin-rich lamellar region after lignin removal by holopulping treatment, in good agreement with the region enclosed by the dashed curve in figure 4(C). Similar observations were made concerning the removal of the lignin in the lamellar region in a previous study by Ragauskas *et al* [27]. Morphological changes can be correlated to chemical changes in the cell wall [3, 27] as has been verified using spectroscopy and chemical analysis techniques [27] on the bulk samples. The changes we observe in the lamellar region of the cross section of holocellulose poplar in figures 4 and 5 are consistent with the Fourier transform infrared FTIR spectroscopy and carbohydrate analysis performed by Jung *et al* [27], where a decrease in S-and G-lignin units was measured for holocellulose. The complexity of the systems requires the use of complementary processes to obtain qualitative and quantitative information on the structure and composition of the cell wall. Time-of-flight secondary ion mass spectrometry (ToF-SIMS) [27] and coherent Raman scattering imaging [42] are also being investigated for simultaneous chemical and morphological characterization of biomass. However, the resolution of these techniques is limited and determining the distribution of cellulose, hemicellulose and lignin within the cell wall remains an important challenge to instrumentation. With respect to high resolution (sub-100 nm) characterization, the physical content of the information obtained with MSAFM can provide valuable information on the role of lignin or cellulose in the stiffness/rigidity/cohesion of the wall [37, 22, 27]. The cell wall thickness changes may relate to the collapse of the cell wall when dried after holocellulose treatment. Furthermore, the MSAFM images of the holocellulose sample obtained simultaneously reveal the complex structure of the surface of the remaining material. The results are presented in figure 6. Although the commonly encountered AFM tip-related artifacts associated with the steep height variations in the morphology of the samples partially remain observable here, MSAFM clearly facilitates the localization of areas, such as the middle lamella and cell corner regions, where the chemical treatment affected the cell walls, which is not always possible to determine with optical or electron microscopy. This technique also helps differentiate the substrate (in this case a glass slide) from the plant sample. The MSAFM image in figure 6 was acquired using the synthesized mode $|1_s1_p\rangle$ (corresponding to nanomechanical sum frequency generation) using the excitation parameters $f_{|1_s0_p\rangle} = 200$ kHz and $R_{|1_s0_p\rangle} = 1\ V_{pp}$ for the substrate, and $f_{|0_s1_p\rangle} = 50$ kHz and $R_{|0_s1_p\rangle} = 2\ V_{pp}$ for the probe. We note that the extent to which surface versus subsurface features are resolved in MSAFM will depend on the particular mode utilized. In the case of complex samples the differentiation among the depth of subsurface information, beyond what may be gathered based on visual inspection, will require careful comparison of the various amplitude and phase images in conjunction with a calibration scheme. However, even at this early maturation level, from the images shown the potential usefulness of the application of MSAFM to plant cells is noteworthy for the detection of heterogeneities within the cell walls.

5. Conclusion

The work presented here constitutes a new approach to biomass characterization using MSAFM, a novel high resolution surface and subsurface imaging method. It can therefore be stated that, for the investigated samples, that is, cross sections of fresh poplar and poplar cross sections subjected to the chemical processes associated with holopulping, the various synthesized modes can help determining the effect of pretreatment on the plant cell wall in order to overcome recalcitrance. The preliminary results on *Populus* samples demonstrate that the proposed MSAFM as a high resolution, label-free, noninvasive imaging technique can be valuable in the study of plant cells. Differences between fresh and holopulped (sodium chlorite holopulp) samples were revealed and quantified. The observed changes in the lamellar region of the holocellulose poplar cross section are consistent with previous work reporting the decrease in S-and G-lignin units in holocellulose. The use of complementary means to investigate the structure and the composition of the plant cell wall contributes to a deeper understanding of the mechanisms at play in recalcitrance. In addition, topographic imaging by AFM was shown to identify the regions of the cross sections affected by the holopulping treatment, and therefore allowed a comparison of the thickness of the cell walls before and after chemical treatment. The ultrasonic-based nanomechanical imaging provided new details of the substructure of the plant cell wall that cannot be achieved with conventional AFM. This modality of AFM yields a new map of the mechanical properties of the plant cell walls where unique features within native and treated plant cell walls could be observed. Naturally, as with the emergence of any new dynamic modality, additional measurements are warranted for the further interpretation of the observed cell structures. The results presented here establish the potential of MSAFM to impact biology by unveiling the structure of complex natural systems at the subcellular level, which is of tremendous importance for the future of biofuel research. Capitalizing on this new

capability, a more involved and systematic characterization of the effects of the successive chemical treatments involved in the decomposition process can be envisioned, as well as the study of other steps involved in the biomass-to-ethanol conversion process, such as enzymatic hydrolysis or fermentation. As the prospect of lignocellulosic biomass for biofuel production is tightly linked to extraction of the sugars necessary for fermentation into ethanol, techniques that can map the ultrastructure of the cell wall as a result of evolving reaction parameters (for instance, temperature, reaction time or acid concentration) are of great interest. Thus, MSAFM has the potential to provide insight in the effort to (1) develop new or improved delignification processes and (2) engineer plants dedicated to biofuel production.

Acknowledgments

This research was sponsored by the Oak Ridge National Laboratory (ORNL) BioEnergy Science Center (BESC). The BioEnergy Science Center is a US Department of Energy (DOE) Bioenergy Research Center supported by the Office of Biological and Environmental Research in the DOE Office of Science. ORNL is managed by UT-Battelle, LLC, for the US DOE under contract DE-AC05-00OR22725.

References

[1] Neuman K C and Nagy A 2008 Single-molecule force spectroscopy: optical tweezers, magnetic tweezers and atomic force microscopy *Nature Methods* **5** 491–505
[2] Muller D J and Dufrene Y F 2008 Atomic force microscopy as a multifunctional molecular toolbox in nanobiotechnology *Nature Nanotechnol.* **3** 261–9
[3] Tetard L, Passian A, Farahi R H, Kalluri U C, Davison B H and Thundat T 2010 Spectroscopy and atomic force microscopy of biomass *Ultramicroscopy* **110** 701–7
[4] Lynd L R *et al* 2008 How biotech can transform biofuels *Nature Biotechnol.* **26** 169–72
[5] Sun Y and Chang J 2002 Hydrolysis of lignocellulosic material for ethanol production: a review *Bioresource Technol.* **83** 1–11
[6] Himmel M 2008 *Biomass Recalcitrance* (Oxford: Blackwell)
[7] Ding S-Y, Himmel M and Xie X S 2008 Identify molecular structural features of biomass recalcitrance using nondestructive microscopy and spectroscopy *Microsc. Microanal.* **14** 1494–5
[8] Sannigrahi P, Ragauskas A J and Tuskan G A 2010 Poplar as a feedstock for biofuels: a review of compositional characteristics *Biofuels, Bioprod. Biorefining* **4** 209–26
[9] Garcia R, Margerle R and Perez R 2007 Nanoscale compositional mapping with gentle forces *Nature Mater.* **6** 405–11
[10] Lozano J R and Garcia R 2008 Theory of multifrequency atomic force microscopy *Phys. Rev. Lett.* **100** 076102
[11] Tetard L, Passian A, Venmar K T, Lynch R M, Voy B H, Shekhawat G, Dravid V P and Thundat T 2008 Imaging nanoparticles in cells by nanomechanical holography *Nature Nanotechnol.* **3** 501–5
[12] Tetard L, Passian A and Thundat T 2010 New modes for subsurface atomic force microscopy through nanomechanical coupling *Nature Nanotechnol.* **5** 105–9
[13] Tetard L, Passian A, Eslami S, Jalili N, Farahi R H and Thundat T 2011 Virtual resonance and frequency difference generation by van der Waals interaction *Phys. Rev. Lett.* **106** 180801
[14] Garcia R 2010 *Amplitude Modulation Atomic Force Microscopy* (Weinheim: Wiley)
[15] Garcia R 2010 Images from below the surface *Nature Nanotechnol.* **5** 101–2
[16] Ding S-Y and Himmel M E 2006 The maize primary cell wall microfibril: a new model derived from direct visualization *J. Agric. Food Chem.* **54** 597–606
[17] Baker A A, Helbert W, Sugiyama J and Miles M J 2000 New insight into cellulose structure by atomic force microscopy shows the $I\alpha$ crystal phase at near-atomic resolution *Biophys. J.* **79** 1139–45
[18] Yarbrough J M, Himmel M E and Ding S-Y 2009 Plant cell wall characterization using scanning probe microscopy techniques *Biotechnol. Biofuels* **2** 17
[19] Jansen S, Choat B and Pletsers A 2009 Morphological variation of intervessel pit membranes and implications to xylem function in angiosperms *Am. J. Bot.* **96** 409–19
[20] Hamm M, Debeire P, Monties B and Chabbert B 2002 Changes in the cell wall network during the thermal dehydration of alfalfa stems *J. Agric. Food Chem.* **50** 1897–903
[21] Foston M, Hubbell C A, Davis M and Ragauskas A J 2009 Variations in cellulosic ultrastructure of poplar *Bioenergy Res.* **2** 193–7
[22] Harris D, Bulone V, Ding S-Y and DeBolt S 2010 Tools for cellulose analysis in plant cell walls *Plant Physiol.* **153** 420–6
[23] Hu Z, Sykes R, Davis M F, Brummer E C and Ragauskas A J 2009 Chemical profiles of switchgrass *Bioresource Technol.* **101** 3253–7
[24] Liu Y-S, Zeng Y, Luo Y, Xu Q, Himmel M E, Smith S J and Ding S-Y 2009 Does the cellulose-binding module move on the cellulose surface? *Cellulose* **16** 587–97
[25] Lucia L A and Rojas O J 2009 *The Nanoscience and Technology of Renewable Biomaterials* (New York: Wiley)
[26] Schmidt M *et al* 2009 Label-free *in situ* imaging of lignification in the cell wall of low lignin transgenic populus trichocarpa *Planta* **230** 589–97
[27] Jung S, Foston M, Sullard M C and Ragauskas A J 2010 Surface characterization of dilute acid pretreated *Populus deltoides* by ToF-SIMS *Energy Fuels* **24** 1347–57
[28] Liu H, Zhu J Y and Chai X S 2011 *In situ*, rapid, and temporally resolved measurements of cellulase adsorption onto lignocellulosic substrates by UV–vis spectrophotometry *Langmuir* **27** 272–8
[29] Zhu P, Moran-Mirabal J, Walker L and Craighead H 2010 Cellulase enzyme binding to pretreated biomass particles using confocal fluorescence microscopy *Biophys. J.* **98** 449
[30] Zeng Y, Saar B, Friedrich M, Chen F, Liu Y-S, Dixon R, Himmel M, Xie X and Ding S-Y 2010 Imaging lignin-downregulated alfalfa using coherent anti-stokes Raman scattering microscopy *Bioenergy Res.* **3** 272–77
[31] Kolosov O V and Yamanaka K 1993 Nonlinear detection of ultrasonic vibrations in an atomic force microscope *Japan. J. Appl. Phys.* **32** L1095–8
[32] Cuberes M T, Briggs G A D and Kolosov O 2001 Nonlinear detection of ultrasonic vibration of AFM cantilevers in and out of contact with the sample *Nanotechnology* **12** 53–9
[33] Shekhawat G S and Dravid V P 2005 Nanoscale imaging of buried structures via scanning near-field ultrasound holography *Science* **310** 89–92

[34] Passian A, Lereu A L, Yi D, Barhen S and Thundat T 2007 Stochastic excitation and delayed oscillation of a micro-oscillator *Phys. Rev.* B **75** 233403
[35] Tetard L, Passian A, Lynch R M, Voy B H, Shekhawat G, Dravid V P and Thundat T 2008 Elastic phase response of silica nanoparticles buried in soft matter *Appl. Phys. Lett.* **93** 133113
[36] Dixon R 2009 DOE Bioenergy Center Special Issue. The Bioenergy Sciences Center (BFSC) *Bioenerg. Res.* **2** 175–6
[37] Albersheim P, Darvill A, Roberts K, Sederoff R and Staehelin R 2010 *Plant Cell Walls* (New York: Garland Science)
[38] Petridis L and Smith J C 2008 Cellulosic ethanol: progress towards a simulation model of lignocellulosic biomass *J. Phys.: Conf. Ser.* **125** 012055
[39] Schulz B, Lindner R, Petridis L and Smith J C 2009 Scaling of multimillion-atom biological molecular dynamics simulation on a petascale supercomputer *J. Chem. Theory Comput.* **5** 2798–808
[40] Zhang D, Pu Y, Chai X-S, Naithani V, Jameel H and Ragauskas A J 2006 Elucidating carboxylic acid profiles for extended oxygen delignification of high-kappa softwood kraft pulps *Holzforschung* **60** 123–9
[41] Sjöström E and Alen R 1998 *Analytical Methods in Wood Chemistry, Pulping and Papermaking* (Berlin: Springer)
[42] Saar B G, Zeng Y, Freudiger C W, Liu Y-S, Himmel M, Xie X S and Ding S-Y 2010 Label-free, real-time monitoring of biomass processing with stimulated Raman scattering microscopy *Angew. Chem. Int. Ed.* **49** 5476–9